

Basic Study

Morphological alterations and redox changes associated with hepatic warm ischemia-reperfusion injury

Rim Jawad, Melroy D'souza, Lisa Arodin Selenius, Marita Wallenberg Lundgren, Olof Danielsson, Greg Nowak, Mikael Björnstedt, Bengt Isaksson

Rim Jawad, Lisa Arodin Selenius, Marita Wallenberg Lundgren, Olof Danielsson, Mikael Björnstedt, Division of Pathology, Department of Laboratory Medicine, Karolinska Institutet, Stockholm S-141 86, Sweden

Melroy D'souza, Bengt Isaksson, Department of Clinical Science, Intervention, and Technology (CLINTEC), Division of Surgery, Karolinska Institutet, Karolinska University Hospital, Huddinge, Stockholm S-141 86, Sweden

Greg Nowak, Department of Clinical Science, Intervention, and Technology (CLINTEC), Division of Transplantation Surgery, Karolinska Institutet, Karolinska University Hospital, Huddinge, Stockholm S-141 86, Sweden

ORCID number: Rim Jawad (0000-0002-4216-0913); Melroy D'souza (0000-0002-6798-8960); Lisa Arodin Selenius (0000-0002-1148-5897); Marita Wallenberg Lundgren (0000-0003-3256-7063); Olof Danielsson (0000-0002-2558-2401); Greg Nowak (0000-0001-8766-8860); Mikael Björnstedt (0000-0003-2831-3837); Bengt Isaksson (0000-0002-7518-7127).

Author contributions: D'souza M, Nowak G, Björnstedt M and Isaksson B contributed to concept and design; Jawad R, D'souza M and Selenius LA contributed to acquisition of data; Jawad R, D'souza M, Lundgren MW, Danielsson O, Nowak G, Björnstedt M and Isaksson B contributed to analysis and interpretation of data; Jawad R, D'souza M and Selenius LA contributed to drafting of the manuscript; Jawad R, D'souza M, Selenius LA, Lundgren MW, Danielsson O, Nowak G, Björnstedt M and Isaksson B contributed to critical revision of the manuscript for important intellectual content; Jawad R, D'souza M and Selenius LA contributed to statistical analysis.

Supported by Swedish Cancer society (Cancerfonden) and the Swedish Cancer and Allergy fund (Cancer-och Allergifonden).

Institutional review board statement: This study was reviewed and approved by the Regional Ethics Committee for human studies, Stockholm.

Informed consent statement: All biopsy specimens and patient data were taken with informed consent for participation in the

study.

Conflict-of-interest statement: No conflict of interest exists.

Data sharing statement: No additional data available.

Open-Access: This article is an open-access article which was selected by an in-house editor and fully peer-reviewed by external reviewers. It is distributed in accordance with the Creative Commons Attribution Non Commercial (CC BY-NC 4.0) license, which permits others to distribute, remix, adapt, build upon this work non-commercially, and license their derivative works on different terms, provided the original work is properly cited and the use is non-commercial. See: <http://creativecommons.org/licenses/by-nc/4.0/>

Manuscript source: Unsolicited manuscript

Correspondence to: Melroy D'souza, MS, DNB MRCSEd, Department of Clinical Science, Intervention, and Technology (CLINTEC), Division of Surgery, Karolinska Institutet, Karolinska University Hospital, Huddinge, Stockholm S-141-86, Sweden. melroy.dsouza@karolinska.se
Telephone: +46-76-2884290
Fax: +46-85-8582340

Received: May 30, 2017

Peer-review started: June 1, 2017

First decision: July 20, 2017

Revised: August 10, 2017

Accepted: October 15, 2017

Article in press: October 15, 2017

Published online: December 8, 2017

Abstract**AIM**

To study the effects of warm ischemia-reperfusion (I/R) injury on hepatic morphology at the ultrastructural level and to analyze the expression of the thioredoxin (TRX)

and glutaredoxin (GRX) systems.

METHODS

Eleven patients undergoing liver resection were subjected to portal triad clamping (PTC). Liver biopsies were collected at three time points; first prior to PTC (baseline), 20 min after PTC (post-ischemia) and 20 min after reperfusion (post-reperfusion). Electron microscopy and morphometry were used to study and quantify ultrastructural changes, respectively. Additionally, gene expression analysis of TRX and GRX isoforms was performed by quantitative PCR. For further validation of redox protein status, immunogold staining was performed for the isoforms GRX1 and TRX1.

RESULTS

Post-ischemia, a significant loss of the liver sinusoidal endothelial cell (LSEC) lining was observed ($P = 0.0003$) accompanied by a decrease of hepatocyte microvilli in the space of Disse. Hepatocellular morphology was well preserved apart from the appearance of crystalline mitochondrial inclusions in 7 out of 11 patients. Post-reperfusion biopsies had similar features as post-ischemia with the exception of signs of a reactivation of the LSECs. No changes in the expression of redox-regulatory genes could be observed at mRNA level of the isoforms of the TRX family but immunoelectron microscopy indicated a redistribution of TRX1 within the cell.

CONCLUSION

At the ultrastructural level, the major impact of hepatic warm I/R injury after PTC was borne by the LSECs with detachment and reactivation at ischemia and reperfusion, respectively. Hepatocytes morphology were well preserved. Crystalline inclusions in mitochondria were observed in the hepatocyte after ischemia.

Key words: Hepatic ischemia-reperfusion injury; Ischemia reperfusion injury; Warm ischemia-reperfusion injury; Glutaredoxins; Thioredoxins; Electron microscopy; Oxidative stress; Portal triad clamping

© **The Author(s) 2017.** Published by Baishideng Publishing Group Inc. All rights reserved.

Core tip: The complex mechanisms of warm Ischemia reperfusion (I/R) injury in the liver are diverse and have been widely studied but poorly understood. This study aims to investigate the ultrastructural changes at warm I/R injury induced by portal triad clamping. The effects were mainly borne by the liver sinusoidal endothelial cells (LSEC) which detached from the sinusoidal wall after ischemia. Interestingly we found that the LSECs reattached after reperfusion. Hepatocytes were unaffected except for the appearance of crystalline inclusions in the mitochondria. Investigation of redox related proteins showed no changes within our time frame.

Jawad R, D'souza M, Selenius LA, Lundgren MW, Danielsson O, Nowak G, Björnstedt M, Isaksson B. Morphological alterations and redox changes associated with hepatic warm ischemia-reperfusion

injury. *World J Hepatol* 2017; 9(34): 1261-1269 Available from: URL: <http://www.wjgnet.com/1948-5182/full/v9/i34/1261.htm> DOI: <http://dx.doi.org/10.4254/wjh.v9.i34.1261>

INTRODUCTION

Ischemia-reperfusion (I/R) injury is a known cause of tissue damage during liver resection and transplantation with direct impact on patients' postoperative morbidity and mortality^[1,2]. It is a biphasic phenomenon whereby the initial hypoxic damage is compounded upon restoration of blood supply along with oxygen delivery. The mechanisms of injury are complex and have been widely studied but remain poorly understood. Hepatic I/R injury is classified as warm or cold, where warm ischemia occurs when the blood supply to the liver is interrupted during liver resection, transplantation, trauma, and shock. Cold storage ischemia occurs during organ preservation in cold preservation solutions before transplantation^[3]. Although both mechanisms share similarities, there are fundamental differences between warm and cold hepatic I/R injury. Existing knowledge indicates that warm I/R injury inflicts hepatocyte damage, while cold I/R injury is primarily characterized by injury to the sinusoidal endothelial lining^[4].

Blood loss is one of the significant determinants of morbidity and tumor recurrence after hepatectomy^[5]. Portal triad clamping (PTC), also known as the Pringle maneuver, has been one of the most widely used methods to reduce blood loss during hepatic surgery and involves clamping of the hepatic vascular inflow. PTC causes warm I/R injury in the remnant liver, the consequences of which are determined by the duration of clamping and the underlying health status of the liver parenchyma.

While there is vast literature regarding the biochemical and metabolic alterations associated with hepatic I/R injury, studies investigating the cellular and ultrastructural changes occurring in the liver as a result of I/R injury have mainly involved animal models and data from human studies are limited^[6-10].

The ischemic injury occurs as a result of a reduction in blood supply and switching from aerobic to anaerobic metabolism. The initial ischemic insult followed by the sudden oxygen burst upon the reestablishment of vascular flow causes reperfusion injury which to a large extent is ascribed to the production of reactive oxygen species (ROS) and associated cellular injury^[11-13]. There are several proteins involved in ROS scavenging and antioxidant defense. Many are regulated at transcriptional level through binding of nuclear factor (erythroid-derived 2)-like 2 (NRF2)^[14], to the Antioxidant-Response Element (ARE) localized upstream of the promoter of these genes. By the same mechanism, *Nrf2* regulates glutamate-cysteine ligase (GCLC) and cysteine/glutamate antiporter (xCT), which are essential for glutathione (GSH) synthesis. GSH maintains the cellular redox balance and is considered

as one of the most important cellular antioxidants^[15,16]. Thioredoxin (TRX) and glutaredoxin (GRX) are two intricate reduction systems belonging to the thioredoxin superfamily of proteins and are ubiquitously expressed in all cell types^[17-19]. There is a lack of information on the involvement of these redox systems in hepatic I/R injury.

The present study aimed at investigating the effects of warm I/R injury induced by PTC in the human liver at the ultrastructural level, determining the degree and character of hepatocyte damage, and the sinusoidal endothelial lining. In addition, the impact of I/R injury on redox proteins was studied, in particular the TRX and GRX systems.

MATERIALS AND METHODS

Patients

Eleven patients (8 men and 3 women), undergoing liver resection for differing indications, but without preoperative clinical or biochemical signs of chronic liver disease, were included in the study. Seven of the patients had colorectal liver metastases and all of them had received preoperative chemotherapy. Two patients had melanoma metastases to the liver and one had metastases from a bowel carcinoid. One patient was operated because of a suspected hepatocellular carcinoma, which on final histopathology turned out to be an inflammatory pseudotumor. The study protocol conformed to the ethical guidelines of the 1975 Declaration of Helsinki and was approved by the Regional Ethics Committee for human studies, Stockholm, Sweden. All patients were informed orally and in writing and gave written consent.

Study protocol and biopsy acquisition

Laparotomy was performed by a right subcostal incision with an upper midline extension and the falciform ligament then divided. The hepatoduodenal ligament was isolated and a PTC then performed by placing a soft cloth tape around the porta hepatis over which a rubber tubing was then slid. With a hemostat, the rubber tubing was adjusted to constrict the vessels in the porta hepatis. The liver was not manipulated during the experimental time period. One wedge biopsy and two needle biopsies (with a Tru-Cut needle) were taken at three time-points; Baseline (just before the application of PTC), post-ischemia (after 20 min of PTC) and post-reperfusion (after 20 min of reperfusion). The needle biopsies were immediately transferred to the required buffers as detailed below before being stored at 4 °C for further analyses. The wedge biopsies were immediately transferred to vials and flash-frozen in liquid nitrogen and stored at -70 °C until analysis. The liver resection was then carried out as planned.

Transmission electron microscopy

The needle biopsies were fixed in 2% glutaraldehyde, 1% paraformaldehyde in 0.1 mol/L phosphate buffer,

pH 7.4 for 10 min at room temperature and then stored at 4 °C. The samples were washed with 0.1 mol/L phosphate buffer, pH 7.4 and then postfixed for 2 h in 2% osmium tetroxide, 0.1 mol/L phosphate buffer, pH 7.4 at 4 °C. Dehydration was performed in ethanol, followed by acetone and the tissue samples were embedded in LX-112. Sections of approximately 70 nm were prepared by an ultramicrotome (Leica EM UC 6). Uranylacetate was added to the sections for contrast followed by lead citrate. A transmission electron microscope (Tecnai 12 Spirit Bio TWIN) was used at 100 kV for examination of the sections and a Veleta[®] camera used for capturing digital images. Assessment of the electron microscopy (EM) findings included evaluation of the cellular architecture, hepatocyte morphology, sinusoids and bile canaliculi.

Morphometric image analysis

NIS Elements Basic Research software was used for quantification analysis of the sinusoids in the electron micrograph images. Pixel length measurements were applied on the sinusoidal endothelial lining surrounding vessels. The number of pixels was determined on one representative sinusoid for each patient and time point, and the length of the endothelial lining was correlated to the length of the entire sinusoid. The retrieved pixel value was related to actual μm for comparison between different images.

Immunoelectron microscopy

Needle biopsies were fixed in 3% paraformaldehyde in 0.1 mol/L phosphate buffer and rinsed in 0.1 mol/L phosphate buffer with subsequent addition of 2.3 mol/L sucrose and subsequently frozen in liquid nitrogen. An ultramicrotome (Leica EM UC 6) was used for the sectioning on carbon-reinforced formvar coated, 50 mesh Nickel grids. The grids were placed on drops of 0.1 mol/L phosphate buffer, 2% BSA, 2% Fish gelatin. Primary antibodies of TRX1 and GRX1 were applied on the sections (GRX1 1:5, TRX1 1:10, own production as described previously^[20], in 0.1 mol/L phosphate buffer, 0.1% BSA, 0.1% gelatin) overnight in a humidified chamber at room temperature. The sections were rinsed with the same buffer and detection of primary antibodies was achieved by protein A with 10 nm gold at a dilution of 1:100. A second wash of the sections was performed before fixation in 2% glutaraldehyde. Contrast was attained by 0.05% uranylacetate and sections were embedded in 1% methylcellulose. A transmission electron microscope (Tecnai G2 Bio TWIN) was used for examination and digital images captured by a Veleta camera[®]. Quantification of the staining was performed on 5 hepatocytes in close proximity to vessels for each tissue section. The number of gold particles in the cytosol and the nuclei were recorded.

RNA purification, cDNA synthesis and qPCR

The fresh frozen wedge biopsies (approximately 10

Table 1 Patient demographics

Patient (gender/age)	Diagnosis	Resection performed	Preoperative chemotherapy	Peak AST, μ kat/L	Peak ALT, μ kat/L	Day of enzyme peak (AST, ALT), (d)	Peak bilirubin, μ mol/L, (d)	Fibrosis (stage)	Inflammation	Steatosis
P1 (M/75)	mCRC	Atypical resection	Yes	4.39	2.23	1	24 (1)	1	0	1
P2 (F/71)	mCRC	Multiple resections	Yes	23.05	21.93	2	53 (1)	1	0	2
P3 (M/39)	Inflammatory pseudotumor	Extended right hepatectomy	No	4.19	4.81	1	41 (1)	-	-	1
P4 (M/75)	Malignant melanoma metastasis	Multiple atypical resections	Yes	2.32	1.90	1	12 (2)	1	0	1
P5 (M/63)	mCRC	Bisegmentectomy	Yes	6.25	7.03	2	16 (1)	1	0	1
P6 (F/78)	Carcinoid metastasis	Left hepatectomy	No	3.73	2.89	1	20 (1)	1	0	1
P7 (F/61)	mCRC	Right hepatectomy	Yes	7.14	6.11	1	14 (1)	1	0	0
P8 (M/55)	Malignant melanoma metastasis	Right hepatectomy	No	7.90	8.84	2	48 (2)	0	0	2
P9 (M/68)	mCRC	Right hepatectomy + atypical resection	Yes	3.85	1.91	1	82 (8)	3-4	2	1
P10 (M/37)	mCRC	Right hepatectomy	Yes	6.71	3.96	2	33 (2)	1	0	0
P11 (M/58)	mCRC	Right hepatectomy + atypical resection	Yes	11.16	9.28	1	53 (2)	1	0	3

Steatosis was defined as 1: Mild (< 33%); 2: Moderate (33%-66%); 3: Severe (> 66%). Fibrosis was defined as Stage 1: Portal fibrosis; Stage 2: Periportal fibrosis; Stage 3: Septal fibrosis; and Stage 4: Cirrhosis. mCRC: Metastatic colorectal cancer.

mg) were homogenized and lysed using a TissueLyser LT with RLT plus lysis buffer (Qiagen). RNeasy Plus Mini Kit (Qiagen) was used for RNA purification according to the manufacturer's instructions, and RNA concentration determination was performed on a NanoDrop ND 100 Spectrophotometer (Saveen Werner). In order to validate the purity and quality of the RNA, Experion Automated Electrophoresis System with Experion RNA StdSens Analysis Kit (BIO-RAD) was used according to manufacturer's protocol. The mRNA quality was assessed for all samples and 6 out of 11 patients had good quality of samples from all time points.

For cDNA synthesis, 2 μ g RNA was subjected to reverse transcription by Omniscript RT kit (Qiagen) according to manufacturer's instructions. Twenty-50 ng cDNA/reaction was used for qPCR in a BIO-RAD iCycler (BIO-RAD). Forward and reverse primers were designed *via* primer BLAST and Ape and purchased from Invitrogen (primer details in Supplementary Table 1). The genes of interest were isoforms of thioredoxins (*TXN*) and glutaredoxins (*GLRX*) and also the gene of *xCT* and *NRF-2*, which are *SLC7A11* and *NFE2L2* respectively. The operation setting for qPCR instrument was the following: 50 °C for 2 min, 95 °C for 2 min with 40 amplification cycles of denaturation at 95 °C for 15 s. Annealing and elongation temperatures of 60 °C, 66 °C or 55 °C were used, depending on the gene of interest, during 30 s. The $2^{-\Delta\Delta CT}$ method was used for quantification by normalizing the CT values against the housekeeping gene β -actin and retrieving fold change relative to the chosen control. A cut off value of 32 cycles was chosen and all primers were optimized for an efficiency of 90%-105%.

Statistical analysis

The statistical analysis was performed using GraphPad

Prism 6.0 software. The non-parametric Friedman test followed by Dunn's *post-hoc* test was used for the analysis of endothelial lining, gene expression data, and immunogold staining data. A *P* values of less than 0.05 was considered to be significant.

RESULTS

Patients

The median age of the patients was 68 (range 39-78) years. Light microscopy evaluation of tissue blocks collected for clinical routine diagnostics from macroscopically non-tumorous liver parenchyma revealed no major histological differences in the surgical specimens from the majority of patients. However, one patient had severe fibrosis, suspicious for cirrhosis (stage 3-4) combined with inflammation of grade 1-2 as defined by Batts and Ludwig^[21]. Two patients had moderate steatosis (defined as 33%-66% of hepatocytes affected). Furthermore, one patient had pronounced steatosis (> 67% of hepatocytes affected). The relevant patient data has been summarized in Table 1.

Ultrastructural examination

At baseline the biopsies exhibited typical hepatic organization with normal hepatocyte and liver sinusoidal endothelial cell (LSEC) morphology. The hepatocytes had a normal appearance, intact plasma membranes, and large numbers of mitochondria without any discernible morphological aberrations at this point. The presence of lipofuscin lipid lysosomes was observed in most liver sections (Table 2). The morphology of the Space of Disse showed hepatocytes with intact microvilli extensions and normal fenestrated LSECs lining the

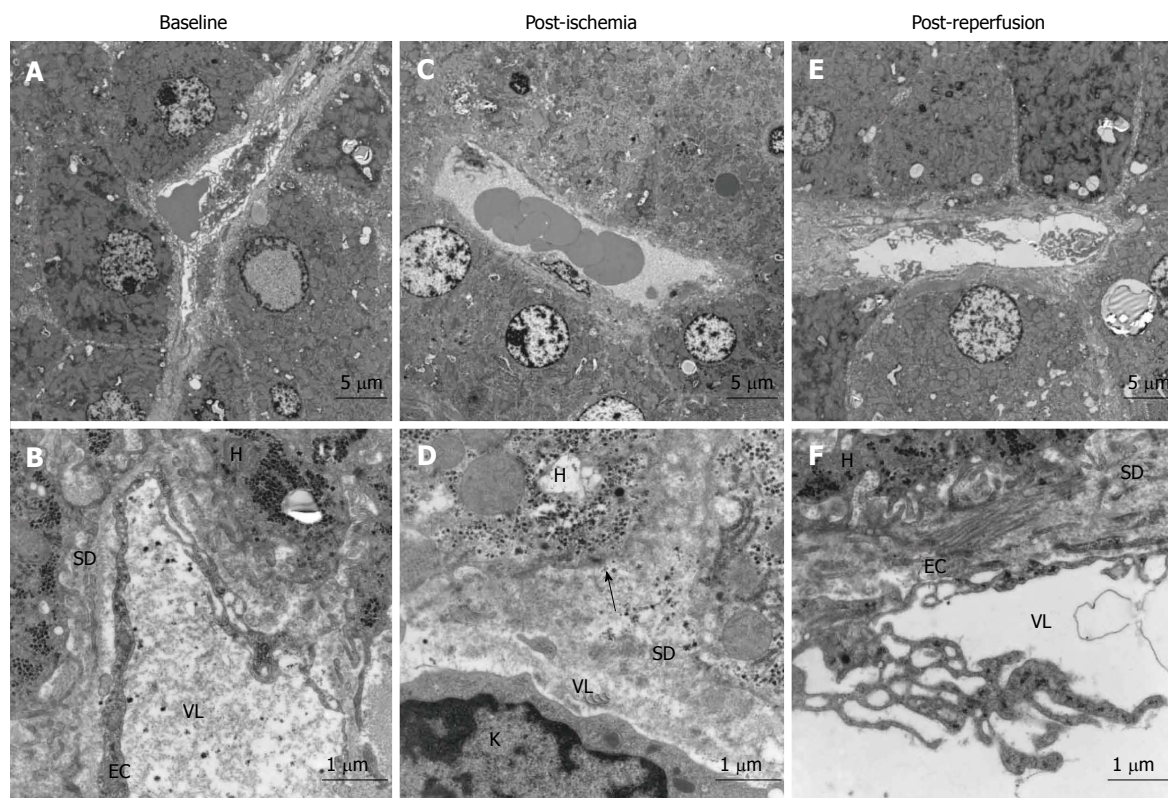


Figure 1 Morphological changes in liver before and after ischemia and reperfusion, transmission electron micrographs of representative images of liver sections from one patient. A: Baseline, before induction of ischemia, shows the normal state of liver morphology at a cellular level; B: Morphology of a sinusoid with neighbouring hepatocytes 20 min after ischemia; C: Representative image of sinusoid and hepatocytes 20 min after reperfusion; D: Endothelial lining of a sinusoid with hepatocyte microvilli; E: Morphology of the Space of Disse post-ischemia; F: Morphology of the space of disse post-reperfusion. SD: Space of disse; H: Hepatocyte; EC: Endothelial cells; VL: Vessel lumen; K: Kupffer cell. Arrow shows the absence of hepatocyte microvilli.

Table 2 Quantitative summary of ultrastructural changes studied by endothelial morphology, (n) patients out of total (11) patients

	Baseline	Post-ischemia	Post-reperfusion
Disruption of endothelium	2/11	10/11	2/11
Endothelial activation	4/11	3/11	9/11
Mitochondrial inclusions in hepatocytes	1/11	6/11	7/11
Lipids, lipofuscin	10/11	10/11	10/11

sinusoids (Figure 1A and D).

The most noticeable change post-ischemia was a disruption of the LSEC lining (Figure 1B and E) in 10 out of 11 patients (Table 2). Apparent changes were seen in the space of Disse where the hepatocyte microvilli decreased in number and were in some cases undetectable (Figure 1E). There were no signs of hepatocyte plasma membrane rupture in either the ischemic or reperfused states. The hepatocytes exhibited some condensed nuclear chromatin but otherwise preserved hepatocyte morphology (Figure 1). In seven out of eleven patients, the hepatocyte mitochondria exhibited aggregates, so-called crystalline inclusions post-ischemia (Figure 2 and Table 2). These inclusions were accompanied by dilated mitochondria, both round and elongated types.

There was a reactivation of the LSECs with pseudopod-like extensions appearing from the cells' surface (Figure 1F and Table 2) post-reperfusion. The hepatocyte microvilli returned to their normal state within the space of Disse. LSEC apoptosis and phagocytosis by Kupffer cells was noticed in some sections. Hepatocyte morphology remained normal and the mitochondrial crystalline inclusions were persistent.

Morphometric analysis of endothelial cell lining loss

In order to evaluate the apparent loss and re-growth of the LSEC lining, quantitative image analysis was performed. This was expressed as a percentage of intact LSEC lining of the total length of the hepatic sinusoid. There was a quantitatively significant reduction in the lining between baseline and post-ischemia ($P = 0.0003$) (Figure 3). However, there was no difference between the baseline level and the post-reperfusion level, indicating a recovery of the LSEC lining post-reperfusion.

Gene expression analysis of redox regulating systems

To study the effects on expression of redox proteins during I/R, relative mRNA expression was investigated for genes implicated in the defense against oxidative stress. The gene expression of *NFE2L2* and *SLC7A11*, coding for the redox regulatory proteins NRF-2 and

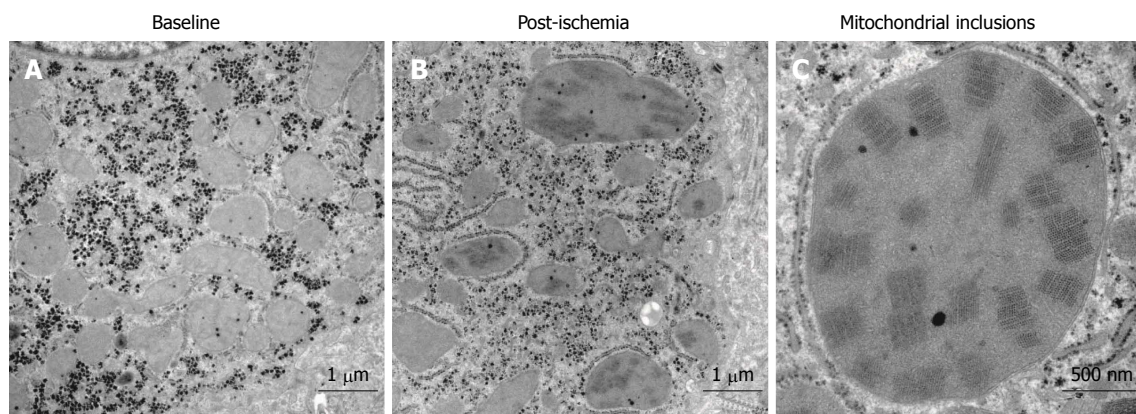


Figure 2 Crystalline mitochondrial inclusions. A: Baseline, before induction of ischemia, shows hepatocyte mitochondria with normal appearance; B: Post-ischemia, showing mitochondria with the crystalline inclusions and a few dilated mitochondria; C: Mitochondrial inclusions, close-up of a single mega-mitochondrion showing the inclusions post-ischemia.

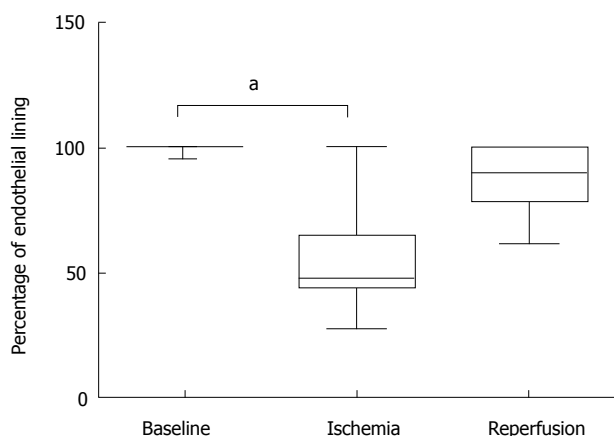


Figure 3 Morphometric analysis of endothelial lining. The percentage of attached endothelial lining along sinusoidal walls was quantified using network information services elements Basic Research Software. Statistical analysis was performed in Graphpad Prism, and differences were determined by the non-parametric Friedman test followed by Dunn's *post-hoc* test ($P < 0.01$). Baseline: Before induction of ischemia; Ischemia: Twenty minutes of ischemia; Reperfusion: Twenty minutes after reperfusion.

xCT, were investigated along with the TRX family of proteins. There were no differences post-ischemia or post-reperfusion compared with baseline (Table 3) of the investigated genes.

Immunoelectron microscopy redox proteins

Immunogold staining for GRX1 and TRX1 was performed in order to study if a translocation of the proteins occurred during I/R. There were no significant changes in the amount of TRX1 either in the nuclei or the cytosol of the hepatocytes during I/R (Figure 4). However, the total amount of TRX differed in the hepatocytes between the time points, and during ischemia the level of TRX decreased in five patients, remained unaffected in three, and increased in two patients (Table 4). The levels of GRX1 did not change in any of the patients during I/R (Figure 4).

DISCUSSION

PTC is an effective method to reduce blood loss

during liver resections but is used very selectively in routine clinical practice^[22]. In general, the extent of I/R injury depends on the duration and magnitude of the ischemia. This study used PTC to investigate ultrastructural changes associated with warm I/R injury. PTC was carried out for a fixed amount of time in all patients and the liver was not manipulated during the experimental procedure and biopsy acquisition. Thus, controlled experimental conditions were established in order to obtain reliable and comparable data. Since PTC is carried out routinely with a 20 min application time, ethical considerations did not permit a more extensive study. The short ischemia time and defined time points of biopsy acquisition thus limited the experimental scope of this study. The findings, however, provide data from human, eventually facilitating our understanding of the complex pathological alterations associated with warm hepatic I/R injury.

Hepatocytes and the LSECs are the cell types most sensitive to I/R injury. In our study, the most noticeable finding in post-ischemia liver biopsies was the loss of the LSEC lining, which was seen in 10 of 11 patients. This finding was significant as shown by the morphometric analysis. According to the current knowledge, based mainly on animal studies, hepatocytes are more sensitive to warm ischemia and LSECs to cold ischemia^[4,23]. Detachment of these specific cells has been previously seen in cold ischemia models in rat^[24,25]. On the other hand one animal study reported that LSEC death may precede hepatocyte death in warm I/R injury^[26]. Here we show, in the human setting, that the LSECs bore the major impact of warm ischemia, visualized by signs of endothelial cell disruption.

Another striking finding in this study was the formation of pseudopod-like projections from the LSEC surface which has been interpreted as a reactivation or reattachment of the LSECs as a response to reperfusion. This was found in 9 of 11 patients and became evident already after 20 min of reperfusion. This suggests that structural loss of LSEC may be reversible when the duration and magnitude of warm

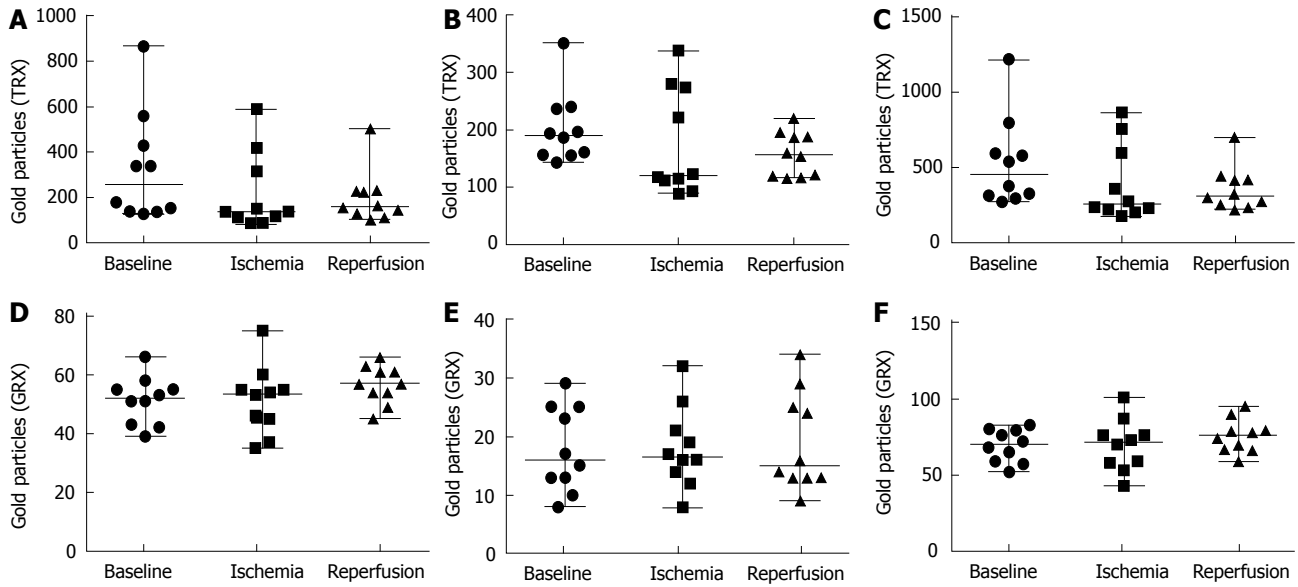


Figure 4 Quantification of immunogold staining. Number of gold particles of 5 hepatocytes for each time point and patient were recorded. A-C: Values from the TRX immunogold staining where A: Quantification of TRX in the cytosol; B: Quantification of TRX in the nuclei; C: Total value of TRX both in cytosol and nuclei; D-F: Values from the quantification of GRX immunogold staining where D: Quantification of GRX in the cytosol; E: Quantification of GRX in the nuclei; F: Total value of GRX both in cytosol and nuclei. Baseline: Before induction of ischemia; Ischemia: Twenty minute of ischemia; Reperfusion: Twenty minute after reperfusion.

	TNX1	TNX2	TNXR1	TNXR2	GLRX1	GLRX2	GLRX3	GLRX5	NFE2L2	SLC7A11
Ischemia	1.09 ± 0.18	1.14 ± 0.30	1.02 ± 0.28	1.05 ± 0.23	1.19 ± 0.41	1.24 ± 0.46	1.03 ± 0.16	1.20 ± 0.27	0.83 ± 0.15	1.27 ± 1.24
Reperfusion	1.12 ± 0.25	1.31 ± 0.57	0.97 ± 0.33	1.39 ± 0.79	1.12 ± 0.67	1.16 ± 0.43	1.16 ± 0.26	1.18 ± 0.63	1.00 ± 0.44	1.22 ± 0.78

I/R injury is limited. It must be noted, however, that late response to reperfusion was not investigated in this study and secondary phases of injury to the LSECs are therefore unknown, if there are any. In a rat model of liver transplantation cold preservation of donor organs resulted in detachment of LSECs followed by some reattachment after reperfusion^[27]. To our knowledge, this phenomenon has never been reported after warm ischemia.

We observed that the hepatocytes lost microvilli in the space of Disse after PTC and some had condensed nuclear chromatin. Furthermore, hepatic mitochondria were dilated and showed the presence of post-ischemic crystalline inclusions which prevailed after reperfusion. Consistent with previous reports, the inclusions almost exclusively appeared in dilated mitochondria^[28]. Apart from these findings the overall morphology of hepatocytes was remarkably well preserved. This is in consistency with an earlier report that has shown that the hepatic ultrastructure was unaffected after intermittent PTC, indicating that the tissue might recover from the injury^[29].

It is known that early hypoxic changes of the hepatocytes can be detected from the morphological alterations of mitochondria^[30]. Mitochondrial crystalline inclusions are commonly seen in early alcohol and non-alcohol related liver diseases and aspirin toxicity^[31-33].

These have been previously described as “para”-crystalline inclusions, however, an optical diffraction study showed that they are true crystals. To date, the composition of these inclusions remains unknown^[34]. The mitochondria of *E. coli* exhibit crystalline inclusions visually similar to these and may arise from copolymerization of the protein Dps to the bacterial DNA as a protective response against oxidative and nutritional stress^[35]. Mitochondrial inclusions could thus be an evolutionarily preserved event and adaptive response to the ischemic state rather than an occurrence secondary to the injury.

Previous studies on oxidative stress in I/R have demonstrated an activation of the transcription factor NRF-2, which regulates a number of redox proteins, including the TRX family of proteins^[15,36]. In our study PTC was used as a model of oxidative stress for studying redox proteins from the TRX family and their alterations in I/R injury. However, no changes on the mRNA levels of the redox proteins could be detected during the 20 min of PTC. Immunogold staining for TRX1 and GRX1 showed no changes in the hepatic GRX1 levels, but the levels of TRX1 present in the hepatocytes varied between the time points, suggesting a possible secretion of the protein. Although TRX1 lacks a translocation signal, this protein can be actively secreted through a leaderless

Table 4 Levels of TRX1, evaluated by immunogold staining, total number of gold particles present in five hepatocytes

Patient	Baseline	Post-ischemia	Post-reperfusion
P1	794	357	414
P2	310	202	323
P3	1217	235	219
P4	373	176	298
P5	324	231	232
P6	269	273	443
P7	575	569	252
P8	294	221	699
P9	535	863	417
P10	590	755	272

secretory pathway that is independent of the classical endoplasmic reticulum-Golgi pathway^[37]. These findings could support a tentative role for the TRX family of proteins in warm I/R injury, however further studies are needed to elucidate this.

We conclude that in a human experimental model of warm I/R injury the major effect observed at the ultrastructural level was on the non-parenchymal LSECs while hepatocytes morphology remained relatively intact apart from crystalline inclusions in the mitochondria after ischemia. Alterations that arise may be protective adaptations that to some extent seem to be reversible. In situ protein observations were compatible with a tentative role for the thioredoxin family of proteins in I/R injury.

COMMENTS

Background

Portal triad clamping (PTC) is used during liver surgery to reduce blood loss. Limiting the blood supply in a tissue can cause ischemia reperfusion (I/R) injury to the tissue. The ischemic injury occurs initially with a switch from aerobic to anaerobic metabolism. Sudden oxygen burst upon returned vascular flow causes reperfusion injuries related to the production of reactive oxygen species (ROS).

Research frontiers

Primary endpoints of clinical studies concerning the PTC method has involved measurements of liver function test, duration of hospital stay, and post-operative complications. Hepatic tissue injury at the ultrastructural level has been sparsely studied and never has there been a differentiation between the ischemic and reperfusion state due to complexity arising in study design.

Innovations and breakthroughs

This is the first study that investigates ultrastructural changes as a result of warm I/R injury during surgery at each point of tissue insult in the liver.

Applications

Limiting the extent of tissue injury during surgery is important for the post-operative recovery of the patients. Evaluation of morphological changes as a result of PTC can provide insights for clinicians of their preferred methods. The results indicate that the changes on the ultrastructural level upon 20 min of ischemia are mainly localized in the sinusoids with a detachment of liver sinusoidal endothelial cells and a loss of hepatocyte microvilli in the Space of Disse. Upon reperfusion the sinusoids showed a reappearance of some liver sinusoidal endothelial cells. The hepatocytes displayed normal morphology with the exception of crystalline inclusions in mitochondria.

Terminology

Crystalline inclusions are characterized visually by dark lines in the mitochondria in the electron microscope. The true composition of the inclusions remain unknown, however *E.coli* have been recorded to display them as a means of protecting mitochondrial DNA in response to oxidative stress.

Peer-review

The authors present an interesting study on the microstructural alterations of liver in a warm ischemia-reperfusion setting.

ACKNOWLEDGMENTS

We would like to express our appreciation to Dr. Sougat Misra for his inputs in preparing the manuscript. This study was supported by grants from: The Swedish Cancer Society (Cancerfonden), The Cancer and Allergy fund (Cancer-och Allergifonden), Radiumhemmets forskningsfonder, ALF, and the Jochnick foundation.

REFERENCES

- Zhai Y, Petrowsky H, Hong JC, Busuttill RW, Kupiec-Weglinski JW. Ischaemia-reperfusion injury in liver transplantation--from bench to bedside. *Nat Rev Gastroenterol Hepatol* 2013; **10**: 79-89 [PMID: 23229329 DOI: 10.1038/nrgastro.2012.225]
- Nastos C, Kalimeris K, Papoutsidakis N, Tasoulis MK, Lykoudis PM, Theodoraki K, Nastou D, Smyrniotis V, Arkadopoulos N. Global consequences of liver ischemia/reperfusion injury. *Oxid Med Cell Longev* 2014; **2014**: 906-965 [PMID: 24799983 DOI: 10.1155/2014/906965]
- Klune JR, Tsung A. Molecular biology of liver ischemia/reperfusion injury: established mechanisms and recent advancements. *Surg Clin North Am* 2010; **90**: 665-677 [PMID: 20637940 DOI: 10.1016/j.suc.2010.04.003]
- Mendes-Braz M, Elias-Miró M, Jiménez-Castro MB, Casillas-Ramírez A, Ramalho FS, Peralta C. The current state of knowledge of hepatic ischemia-reperfusion injury based on its study in experimental models. *J Biomed Biotechnol* 2012; **2012**: 298-657 [PMID: 22649277 DOI: 10.1155/2012/298657]
- Kooby DA, Stockman J, Ben-Porat L, Gonen M, Jarnagin WR, Demattee RP, Tuorto S, Wuest D, Blumgart LH, Fong Y. Influence of transfusions on perioperative and long-term outcome in patients following hepatic resection for colorectal metastases. *Ann Surg* 2003; **237**: 860-869; discussion 869-870 [PMID: 12796583 DOI: 10.1097/01.SLA.0000072371.95588.DA]
- Man K, Lo CM, Liu CL, Zhang ZW, Lee TK, Ng IO, Fan ST, Wong J. Effects of the intermittent Pringle manoeuvre on hepatic gene expression and ultrastructure in a randomized clinical study. *Br J Surg* 2003; **90**: 183-189 [PMID: 12555294 DOI: 10.1002/bjs.4027]
- Nadig SN, Periyasamy B, Shafizadeh SF, Polito C, Fiorini RN, Rodwell D, Evans Z, Cheng G, Dunkelberger D, Schmidt M, Self SE, Chavin KD. Hepatocellular ultrastructure after ischemia/reperfusion injury in human orthotopic liver transplantation. *J Gastrointest Surg* 2004; **8**: 695-700 [PMID: 15358330 DOI: 10.1016/j.gassur.2004.04.002]
- Vollmar B, Glasz J, Leiderer R, Post S, Menger MD. Hepatic microcirculatory perfusion failure is a determinant of liver dysfunction in warm ischemia-reperfusion. *Am J Pathol* 1994; **145**: 1421-1431 [PMID: 7992845]
- Moussa ME, Sarraf CE, Uemoto S, Sawada H, Habib NA. Effect of total hepatic vascular exclusion during liver resection on hepatic ultrastructure. *Liver Transpl Surg* 1996; **2**: 461-467 [PMID: 9346693 DOI: 10.1002/lt.500020609]
- Rodriguez AA, LaMorte WW, Hanrahan LM, Hopkins SR, O'Keane JC, Cachecho R, Hirsch EF. Liver viability after ischemia-reperfusion. *Arch Surg* 1991; **126**: 767-772 [PMID: 2039366 DOI: 10.1001/archsurg.1991.01410300113018]

- 11 **Galaris D**, Barbouti A, Korantzopoulos P. Oxidative stress in hepatic ischemia-reperfusion injury: the role of antioxidants and iron chelating compounds. *Curr Pharm Des* 2006; **12**: 2875-2890 [PMID: 16918418 DOI: 10.2174/138161206777947614]
- 12 **Togashi H**, Shinzawa H, Yong H, Takahashi T, Noda H, Oikawa K, Kamada H. Ascorbic acid radical, superoxide, and hydroxyl radical are detected in reperfusion injury of rat liver using electron spin resonance spectroscopy. *Arch Biochem Biophys* 1994; **308**: 1-7 [PMID: 8311441 DOI: 10.1006/abbi.1994.1001]
- 13 **Togashi H**, Shinzawa H, Matsuo T, Takeda Y, Takahashi T, Aoyama M, Oikawa K, Kamada H. Analysis of hepatic oxidative stress status by electron spin resonance spectroscopy and imaging. *Free Radic Biol Med* 2000; **28**: 846-853 [PMID: 10802214 DOI: 10.1016/S0891-5849(99)00280-4]
- 14 **Jaeschke H**, Woolbright BL. Current strategies to minimize hepatic ischemia-reperfusion injury by targeting reactive oxygen species. *Transplant Rev (Orlando)* 2012; **26**: 103-114 [PMID: 22459037 DOI: 10.1016/j.trre.2011.10.006]
- 15 **Sasaki H**, Sato H, Kuriyama-Matsumura K, Sato K, Maebara K, Wang H, Tamba M, Itoh K, Yamamoto M, Bannai S. Electrophile response element-mediated induction of the cystine/glutamate exchange transporter gene expression. *J Biol Chem* 2002; **277**: 44765-44771 [PMID: 12235164 DOI: 10.1074/jbc.M208704200]
- 16 **Ishii T**, Itoh K, Takahashi S, Sato H, Yanagawa T, Katoh Y, Bannai S, Yamamoto M. Transcription factor Nrf2 coordinately regulates a group of oxidative stress-inducible genes in macrophages. *J Biol Chem* 2000; **275**: 16023-16029 [PMID: 10821856 DOI: 10.1074/jbc.275.21.16023]
- 17 **Lillig CH**, Berndt C, Holmgren A. Glutaredoxin systems. *Biochim Biophys Acta* 2008; **1780**: 1304-1317 [PMID: 18621099 DOI: 10.1016/j.bbagen.2008.06.003]
- 18 **Lillig CH**, Holmgren A. Thioredoxin and related molecules--from biology to health and disease. *Antioxid Redox Signal* 2007; **9**: 25-47 [PMID: 17115886 DOI: 10.1089/ars.2007.9.25]
- 19 **Hirota K**, Matsui M, Iwata S, Nishiyama A, Mori K, Yodoi J. AP-1 transcriptional activity is regulated by a direct association between thioredoxin and Ref-1. *Proc Natl Acad Sci USA* 1997; **94**: 3633-3638 [PMID: 9108029 DOI: 10.1073/pnas.94.8.3633]
- 20 **Mollbrink A**, Jawad R, Vlamis-Gardikas A, Edenvik P, Isaksson B, Danielsson O, Stål P, Fernandes AP. Expression of thioredoxins and glutaredoxins in human hepatocellular carcinoma: correlation to cell proliferation, tumor size and metabolic syndrome. *Int J Immunopathol Pharmacol* 2014; **27**: 169-183 [PMID: 25004829 DOI: 10.1177/039463201402700204]
- 21 **Batts KP**, Ludwig J. Chronic hepatitis. An update on terminology and reporting. *Am J Surg Pathol* 1995; **19**: 1409-1417 [PMID: 7503362 DOI: 10.1097/00000478-199512000-00007]
- 22 **Rahbari NN**, Wente MN, Schemmer P, Diener MK, Hoffmann K, Motschall E, Schmidt J, Weitz J, Büchler MW. Systematic review and meta-analysis of the effect of portal triad clamping on outcome after hepatic resection. *Br J Surg* 2008; **95**: 424-432 [PMID: 18314921 DOI: 10.1002/bjs.6141]
- 23 **Peralta C**, Jiménez-Castro MB, Gracia-Sancho J. Hepatic ischemia and reperfusion injury: effects on the liver sinusoidal milieu. *J Hepatol* 2013; **59**: 1094-1106 [PMID: 23811302 DOI: 10.1016/j.jhep.2013.06.017]
- 24 **Holloway CM**, Harvey PR, Mullen JB, Strasberg SM. Evidence that cold preservation-induced microcirculatory injury in liver allografts is not mediated by oxygen-free radicals or cell swelling in the rat. *Transplantation* 1989; **48**: 179-188 [PMID: 2667203 DOI: 10.1097/0007890-198908000-00001]
- 25 **Fratté S**, Gendraul JL, Steffan AM, Kirn A. Comparative ultrastructural study of rat livers preserved in Euro-Collins or University of Wisconsin solution. *Hepatology* 1991; **13**: 1173-1180 [PMID: 2050331 DOI: 10.1002/hep.1840130625]
- 26 **Kohli V**, Selzner M, Madden JF, Bentley RC, Clavien PA. Endothelial cell and hepatocyte deaths occur by apoptosis after ischemia-reperfusion injury in the rat liver. *Transplantation* 1999; **67**: 1099-1105 [PMID: 10232558 DOI: 10.1097/00007890-199904270-00003]
- 27 **Morgan GR**, Sanabria JR, Clavien PA, Phillips MJ, Edwards C, Harvey PR, Strasberg SM. Correlation of donor nutritional status with sinusoidal lining cell viability and liver function in the rat. *Transplantation* 1991; **51**: 1176-1183 [PMID: 2048194 DOI: 10.1097/00007890-199106000-00007]
- 28 **Le TH**, Caldwell SH, Redick JA, Sheppard BL, Davis CA, Arseneau KO, Iezzoni JC, Hespeneide EE, Al-Osaimi A, Peterson TC. The zonal distribution of megamitochondria with crystalline inclusions in nonalcoholic steatohepatitis. *Hepatology* 2004; **39**: 1423-1429 [PMID: 15122772 DOI: 10.1002/hep.20202]
- 29 **Man K**, Liang TB, Lo CM, Liu CL, Ng IO, Yu WC, Fan ST. Hepatic stress gene expression and ultrastructural features under intermittent Pringle manoeuvre. *Hepatobiliary Pancreat Dis Int* 2002; **1**: 249-257 [PMID: 14612278]
- 30 **Lemasters JJ**. V. Necrapoptosis and the mitochondrial permeability transition: shared pathways to necrosis and apoptosis. *Am J Physiol* 1999; **276**: G1-G6 [PMID: 9886971]
- 31 **Manov I**, Motanis H, Frumin I, Iancu TC. Hepatotoxicity of anti-inflammatory and analgesic drugs: ultrastructural aspects. *Acta Pharmacol Sin* 2006; **27**: 259-272 [PMID: 16490160 DOI: 10.1111/j.1745-7254.2006.00278.x]
- 32 **Caldwell SH**, Swerdlow RH, Khan EM, Iezzoni JC, Hespeneide EE, Parks JK, Parker WD Jr. Mitochondrial abnormalities in non-alcoholic steatohepatitis. *J Hepatol* 1999; **31**: 430-434 [PMID: 10488700 DOI: 10.1016/S0168-8278(99)80033-6]
- 33 **Sanyal AJ**, Campbell-Sargent C, Mirshahi F, Rizzo WB, Contos MJ, Sterling RK, Luketic VA, Shiffman ML, Clore JN. Nonalcoholic steatohepatitis: association of insulin resistance and mitochondrial abnormalities. *Gastroenterology* 2001; **120**: 1183-1192 [PMID: 11266382 DOI: 10.1053/gast.2001.23256]
- 34 **Sternlieb I**, Berger JE. Optical diffraction studies of crystalline structures in electron micrographs. II. Crystalline inclusions in mitochondria of human hepatocytes. *J Cell Biol* 1969; **43**: 448-455 [PMID: 5351401 DOI: 10.1083/jcb.43.3.448]
- 35 **Wolf SG**, Frenkiel D, Arad T, Finkel SE, Kolter R, Minsky A. DNA protection by stress-induced biocrystallization. *Nature* 1999; **400**: 83-85 [PMID: 10403254 DOI: 10.1038/21918]
- 36 **Itoh K**, Chiba T, Takahashi S, Ishii T, Igarashi K, Katoh Y, Oyake T, Hayashi N, Satoh K, Hatayama I, Yamamoto M, Nabeshima Y. An Nrf2/small Maf heterodimer mediates the induction of phase II detoxifying enzyme genes through antioxidant response elements. *Biochem Biophys Res Commun* 1997; **236**: 313-322 [PMID: 9240432 DOI: 10.1006/bbrc.1997.6943]
- 37 **Rubartelli A**, Bajetto A, Allavena G, Wollman E, Sitia R. Secretion of thioredoxin by normal and neoplastic cells through a leaderless secretory pathway. *J Biol Chem* 1992; **267**: 24161-24164 [PMID: 1332947]

P- Reviewer: Camara-Lemarrocy C, Losano G **S- Editor:** Cui LJ
L- Editor: A **E- Editor:** Lu YJ





Published by **Baishideng Publishing Group Inc**
7901 Stoneridge Drive, Suite 501, Pleasanton, CA 94588, USA
Telephone: +1-925-223-8242
Fax: +1-925-223-8243
E-mail: bpgoffice@wjgnet.com
Help Desk: <http://www.f6publishing.com/helpdesk>
<http://www.wjgnet.com>

